JOURNAL OF MATERIALS SCIENCE: MATERIALS IN MEDICINE 13 (2002) 1167–1173

Calcium phosphate thin film processing by pulsed laser deposition and *in situ* assisted ultraviolet pulsed laser deposition

V. NELEA*, H. PELLETIER
Laboratoire d'Ingénierie de Surface, Ecole Nationale Supérieure des Arts et Industries, 24 Bld. de la Victoire, F-67084, Strasbourg, France

M. ILIESCU, J. WERCKMANN
Groupe Surfaces Interfaces, Institut de Physique et Chimie des Matériaux, 23, Rue de Lœss, F-67037, Strasbourg, France

V. CRACIUN
Department of Materials Science and Engineering, University of Florida, Gainesville, FL 32611, USA

I. N. MIHAILESCU, C. RISTOSCU
Laser Department, National Institute for Lasers, Plasma and Radiation Physics, PO Box MG-36, RO-76900, Bucharest, Magurele, Romania

C. GHICA
National Institute of Materials Physics, PO Box MG-7, RO-76900, Bucharest, Magurele, Romania
E-mail: nelea@ensais2.u-strasbg.fr; nelea@ifin.nipne.ro

Calcium orthophosphates (CaP) and hydroxyapatite (HA) were intensively studied in order to design and develop a new generation of bioactive and osteoconductive bone prostheses. The main drawback now in the CaP and HA thin films processing persists in their poor mechanical characteristics, namely hardness, tensile and cohesive strength, and adherence to the metallic substrate. We report here a critical comparison between the microstructure and mechanical properties of HA and CaP thin films grown by two methods. The films were grown by KrF* pulsed laser deposition (PLD) or KrF* pulsed laser deposition assisted by *in situ* ultraviolet radiation emitted by a low pressure Hg lamp (UV-assisted PLD). The PLD films were deposited at room temperature, in vacuum on Ti–5Al–2.5Fe alloy substrate previously coated with a TiN buffer layer. After deposition the films were annealed in ambient air at 500–600 °C. The UV-assisted PLD films were grown in (10^{-2}–10^{-1} Pa) oxygen directly on Ti–5Al–2.5Fe substrates heated at 500–600 °C. The films grown by classical PLD are crystalline and stoichiometric. The films grown by UV-assisted PLD were crystalline and exhibit the best mechanical characteristics with values of hardness and Young modulus of 6–7 and 150–170 GPa, respectively, which are unusually high for the calcium phosphate ceramics. To the difference of PLD films, in the case of UV-assisted PLD, the GIXRD spectra show the decomposition of HA in $Ca_2P_2O_7$, $Ca_2P_2O_9$ and CaO. The UV lamp radiation enhanced the gas reactivity and atoms mobility during processing, increasing the tensile strength of the film, while the HA structure was destroyed.
© *2002 Kluwer Academic Publishers*

1. Introduction

The research in the biocompatible materials field was recently strongly targeted to create coatings or thin films of calcium phosphates (CaP) on mechanically resistant support [1]. The purpose of these efforts was to improve the biocompatibility of the titanium and its alloys used in bone implantology.

Due to the very complex structure of bone as an organic–inorganic composite (at micro- and also at macrolevel) a material with function of artificial bone

* Author to whom all correspondence should be addressed. On leave from National Institute for Lasers, Plasma and Radiation Physics, Lasers Department, P.O. Box MG-36, RO-76900, Bucharest, Magurele, Romania.

it is not available. Thus, calcium orthophosphates (CaP) and hydroxyapatite (HA), $Ca_5(PO_4)_3OH$, were continuously studied in order to design and develop a new generation of bioactive and osteoconductive bone prostheses [2].

The excellent bioactivity determined by similar composition and crystallographic structure with the mineral substance of the bone makes HA a challenge to successful bone repair. On the other hand, the using of various CaP phases, which have different rates of bioresorbability, allows fabricating custom prosthetic devices.

Due to relative complex formula of the HA molecule, it is rather difficult to deposit stoichiometric films. Thus, various chemical and physical deposition methods have been applied in order to obtain adherent and stoichiometric HA thin films. The commercial plasma spray technique [3] presents some problems associated with the lack of crystallinity and mixture of phases. However, the main drawback in the growth of ceramic HA and CaP thin films, commonly to majority of the deposition methods, still stay in the poor mechanical characteristics of the films, especially hardness, tensile strength and adherence to the metallic substrate [4].

One of the most promising deposition techniques of CaP films, and which could even replace the actual used method of plasma spray, is the pulsed laser deposition (PLD) [5]. This method has demonstrated the capability to grow stoichiometric and high crystalline layers of various materials. Depending on the deposition parameters, the PLD can create CaP coatings with different phases and chemical composition. The composition and the stoichiometry are a measure of biocompatibility by determining the bioresorbability rate of the CaP coatings. The PLD is a feasible and versatile method to produce systems of layers and multilayers of different bioresorbability rates [6].

It is generally accepted that successful creation of crystalline HA films imperatively demand the use of water vapor atmosphere and substrates kept at rather high temperatures (450–600 °C) during growth [7]. As most of the metallic prostheses are made out of Ti or Ti-based alloy, it is evident that under harsh conditions the Ti surface oxidizes. This is why pulsed laser deposited films exhibit sometimes not very good mechanical properties: the interface between the HA film and the substrate undergoes degradation by inevitably oxidation of the metallic support [8].

In a previous work we have demonstrated that the insertion of a buffer layer of ceramic TiN, ZrO_2, and Al_2O_3 at the HA film-Ti-based alloy substrate interface improves the mechanical features and the adherence of nanocrystalline HA films grown by PLD [9]. The buffer layer acts as an efficient barrier against the diffusion of the Ti atoms or/and ions from substrate to the film. Moreover, the nano-hardness and the mechanical resistance of films deposited on TiN buffer layers can be considerably increased after a high energy ion-beam implantation treatment with Ar^+ ions [10].

It is known that vacuum ultraviolet (VUV) radiation, whose wavelengths are lower than 200 nm, produces the photodissociation of molecular oxygen, resulting in the formation of very reactive species such as ozone and atomic oxygen [11]. Thus, using these gases, the crystallographic properties of the structures of the oxide films could be improved. This has been demonstrated in experiments of rapid oxidation of silicon at low temperature, using halogen, excimer or low-pressure Hg lamps as UV radiation sources [12]. Based on the phenomena involved by the UV irradiation emitted by lamps with the environmental gas and plasma of a typical PLD experiment, a new deposition technique has recently appeared as a hybrid of PLD, namely *in situ* assisted ultraviolet pulsed laser deposition (UV-assisted PLD) [13].

We report here a critical comparison between the microstructure and mechanical properties of HA and CaP thin films grown by these two non-conventional techniques, PLD and UV-assisted PLD.

2. Experimental details

We used a typical PLD installation for the depositions, composed of a KrF* ($\lambda = 248\,\text{nm}, \tau_{FWHM} \geq 20\,\text{ns}$) excimer laser source and a stainless steel vacuum chamber. A low-pressure Hg lamp having a fused silica envelope, which allow $\sim 85\%$ of the emitted 184.9 nm radiation (around 6% of the 25 W output) to be transmitted, was added to the PLD system in order to accomplish the UV-assisted PLD experiments. The lamp is positioned at about 7 cm in front of the substrate, below the target. It was used for *in situ* UV irradiation during the laser ablation-growth process. It was switched on before the deposition process to clean the substrate of organic contaminants.

Pellets pressed from pure HA powder (99.98%, grains $\leq 100\,\mu\text{m}$) were used as targets for laser ablation.

The depositions were made on Ti–5Al–2.5Fe alloys discs previously coated or not with a TiN buffer layer. The PLD films were deposited in vacuum on TiN/Ti–5Al–2.5Fe composite substrate maintained at room temperature. After deposition the films were annealed in ambient air at 500–600 °C. The UV-assisted PLD films were grown in (10^{-2}–10^{-1} Pa) oxygen directly on Ti–5Al–2.5Fe substrates heated at 500–600 °C.

The TiN buffer layers were created also by PLD. To accomplish this we ablate a stoichiometric TiN target in 10^{-1} Pa nitrogen atmosphere. The temperature of the Ti-based substrate was 550–650 °C.

The laser fluence is 1–2J cm^{-2}, while the ablation rate is ~ 0.5 Å/pulse. The thickness of the CaP and HA films varied between 0.5 and 2.5 μm.

The films were structurally characterized by grazing incidence X-ray diffraction (GIXRD), transmission electron microscopy (TEM) and selected area electron diffraction (SAED). The chemical composition (Ca/P film ratio) was determined by energy dispersive spectrometry (EDS). The surface morphology was analyzed by scanning electron microscopy (SEM) and white light confocal microscopy (WLCM). Starting from the microtopographic data recorded by WLCM, the roughness parameters of the film surface were determined. Finally, the mechanical properties of the films were tested by Berkovich nanoindentation.

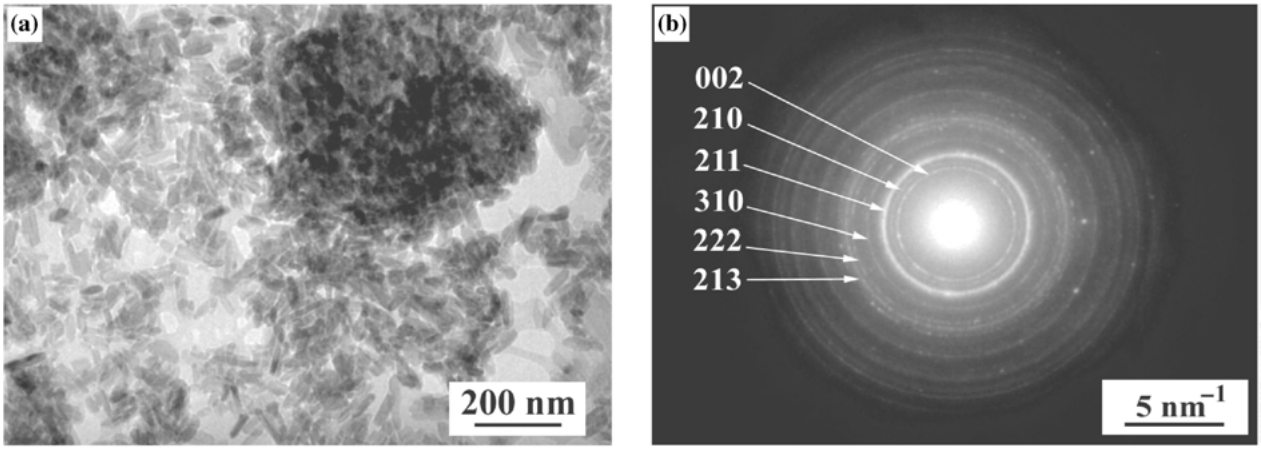

Figure 1 Electron microscopy analyses of the hydroxyapatite powder used for deposition: TEM micrograph (a) and the corresponding SAED pattern (b).

3. Results

3.1. Structural investigations

The TEM investigations were performed on a TEM-SCAN JEOL 200-CX electron microscope at an acceleration tension of 200 keV.

Fig. 1(a) presents the TEM micrograph showing the nano-crystalline structure of the HA powder used for deposition. The image reveals that the powder is formed by crystallites in form of baguettes of about 20 nm wide and 60 nm length sizes. In Fig. 1(b) we show the SAED pattern obtained for the powder. This pattern contains solely diffraction rings characteristic to typical poly-crystalline hydroxyapatite phase (card No. 9-0432 in ASTM-JCPDS).

In Fig. 2 we illustrate the TEM micrograph (Fig. 2(a)) and its characteristic SAED pattern (Fig. 2(b)) obtained for a film grown by PLD on a Ti–5Al–2.5Fe previously coated with a TiN buffer layer. The TEM image shows a nano-crystalline structure of the film similar to that of the powder. The crystallites have a cubic shape with an average size of about 20–30 nm. The SAED pattern is identical to that recorded from the powder, confirming the solely presence of HA in the film.

GIXRD investigations were performed on a Siemens D 500 diffractometer equipped with Soller slits. The incident radiation was CuK_{α} (0.154 nm wavelength). Each sample was analyzed at a grazing incidence angle varying between 0.3° and 1°.

The spectra in Fig. 3 were obtained at an angle of incidence of 0.5°. They correspond to a PLD film deposited on a TiN/Ti–5Al–2.5Fe composite substrate (Fig. 3(a)) and of one deposited by UV-assisted PLD directly on Ti–5Al–2.5Fe substrate (Fig. 3(b)).

In the case of film grown by PLD, the main X-ray diffraction peaks characteristic for the HA phase were observed in the spectrum. This confirms the presence of HA phase in the film. Reflections of (2 0 0) and (2 2 0) crystallographic plains of TiN Osbornite phase (card No. 38-1420 in ASTM-JCPDS) belonging to the buffer layer were also detected.

The recorded spectra (Fig. 3(b)) reveal the presence in the UV-assisted PLD film structure of the following phases: tetra-calcium phosphate (TTCP), $Ca_4O(PO_4)_2$ (card No. 25-1137 in ASTM-JCPDS), dicalcium phosphate phase β (DCP, Whitlockite), $Ca_2P_2O_7$ (card No. 9-0346) and CaO (Lime, card No. 37-1497). These phases seem to be decomposition products from the hydroxyapatite target. However, a small amount of crystalline hydroxyapatite is present in the film: some small diffraction peaks (around 33° in 2θ) are assigned to the XRD pattern of hydroxyapatite (card No. 9-0432 in ASTM-JCPDS).

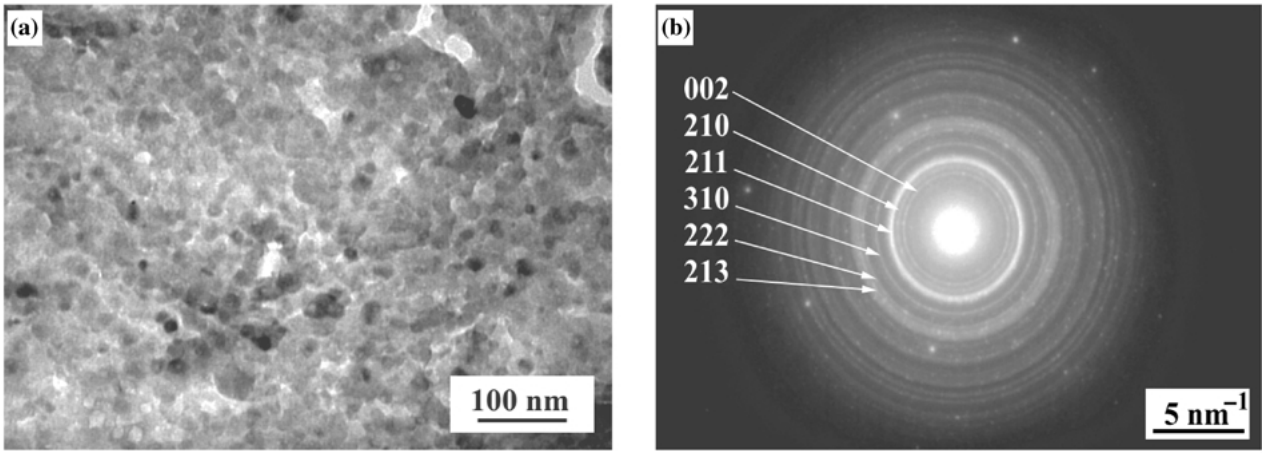

Figure 2 Electron microscopy analyses of a HA films grown by PLD on a TiN/Ti–5Al–2.5Fe composite substrate; TEM micrograph (a) and the corresponding SAED pattern (b).

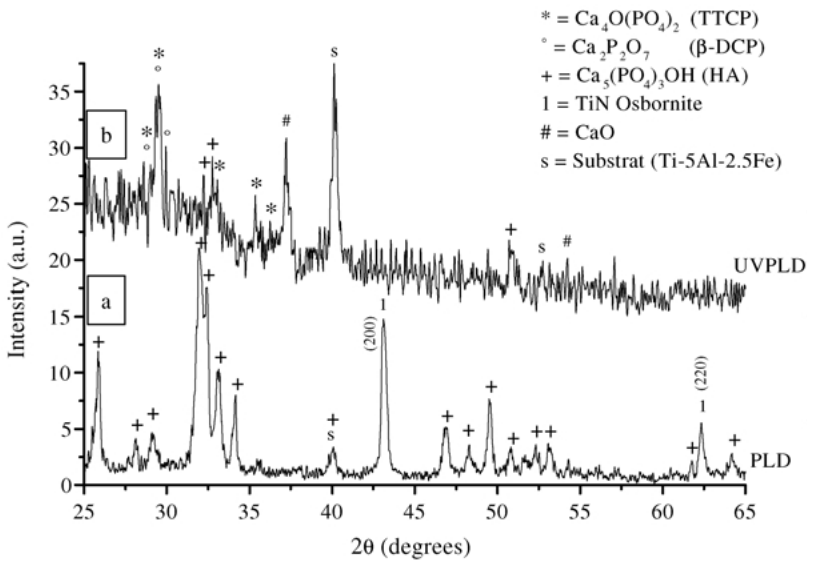

Figure 3 GIXRD pattern obtained at 0.5° incidence angle for PLD (a) and UV-assisted PLD (b) films.

The electron microscopy analyses performed on a fragment of an UV-assisted PLD film is presented in Fig. 4. The SAED pattern (Fig. 4(b)) reveals the electron diffraction rings characteristic to the calcium monoxide, CaO (Lime, card No. 37-1497) which presence in the film structure was detected by GIXRD. A TEM micrograph acquired in this zone representing the CaO nano-crystalline film structure is illustrated in (Fig. 4(a)).

EDS determined the film stoichiometry by obtaining the Ca/P atomic ratio. The analyses were performed using a microprobe electron beam of 14 nm diameter. The Ca/P atomic ratio of the PLD film varies slightly around 1.73, while the values measured for the UV-assisted PLD are between 1.9 and 2.1. The average value ($\sim$ 2), corresponding to a film composition depleted in phosphorous, is identical to that of the TTCP phase, whose presence was detected by GIXRD investigations. The presence in a relatively high amount of CaO phase, determined both by GIXRD and SAED, confirm the diminution in the phosphorus content.

3.2. Morphology analyzes

The scanning electron microscopy investigations were performed on a typical JEOL electron microscope.

Fig. 5 presents the aspect of the surface of a CaP film grown by PLD (Fig. 5(a)) and by UV-assisted PLD (Fig. 5(b)). The films grown by classical PLD present a relatively irregular morphology. Moreover, small formations of material in form of mounds (rises), most probably produced as a result of film recrystallization, are visible on the film surface. We note that these small protuberances, which appear on the film surface, are not inconvenient for a good apposition of the osteoblate cells at the bioceramic coating.

The films grown by UV-assisted PLD seem to be more uniform and smooth. However, micrometric particulates in form of droplets, horseshoes and spirals are distinguished on the surface.

Roughness measurement and micro-topographic data have been obtained using a white light confocal microscope (WLCM) in extended field (Micromeasure CHR® 150, STIL, Aix en Provence, France). The

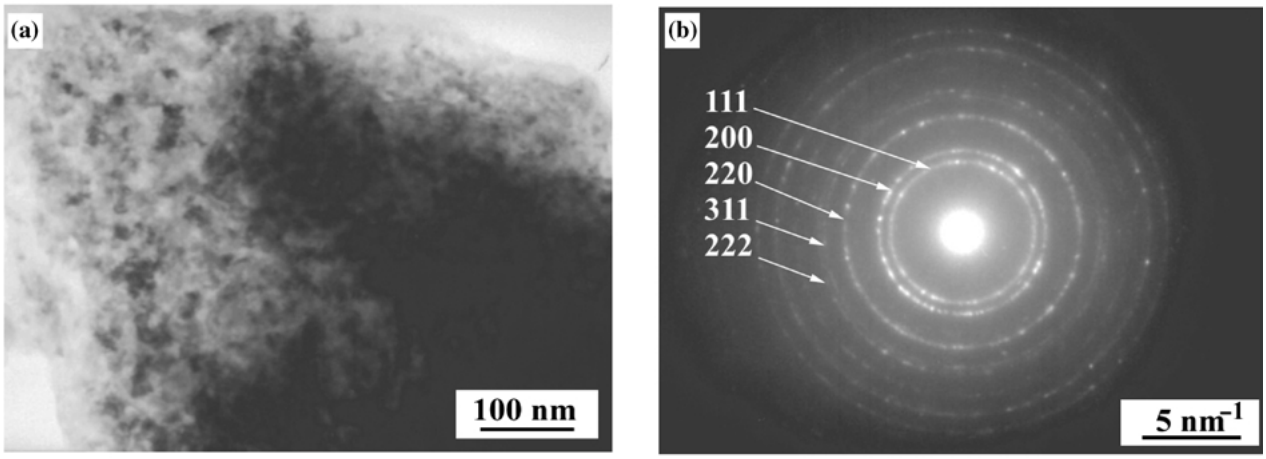

Figure 4 Electron microscopy analyses of a films grown by UV-assisted PLD on a Ti–5Al–2.5Fe substrate; TEM micrograph (a) and the corresponding SAED pattern (b).

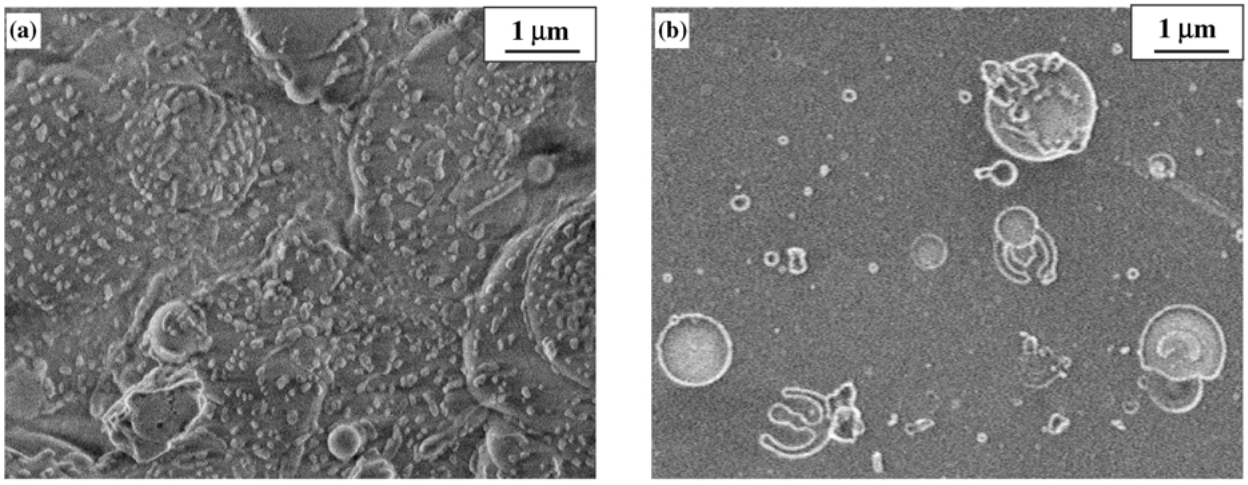

Figure 5 SEM micrographs showing the surface morphology of the films grown by PLD (a) and UV-assisted PLD (b).

TABLE I Roughness parameters of the PLD and UV-assisted PLD films determined by WLCM

Films	Roughness parameters		
	R_q (nm)	R_a (nm)	$R_{\max}$ (nm)
PLD	285	250	450
UVPLD	12.5	10	102

TABLE II Nano-hardness and Young modulus of CaP films grown by PLD and UV-assisted PLD

Film	H (GPa)	H_a (GPa)	E (GPa)	E_a (GPa)
PLD	2.4–3	2.7	90–120	111
UVPLD	6–7.5	7	160–180	170

vertical and lateral resolutions are 0.01 and 2 μm, respectively [14]. From WLCM images, two roughness parameters have been calculated:

a. the standard deviation of the height values (R_q, rms), which is given by:

$$R_q = \sqrt{\frac{1}{L_x}\frac{1}{L_y}\int_0^{L_x}\int_0^{L_y} z^2(x,y)\,dx\,dy} \qquad (1)$$

b. the mean roughness (R_a) calculated as:

$$R_a = \frac{1}{L_x}\frac{1}{L_y}\int_0^{L_x}\int_0^{L_y} |z(x,y)|\,dx\,dy \qquad (2)$$

Here $z(x, y)$ is the surface relative to the mean plane. L_x and L_y were the dimensions in (x, y) plane.

The highest values of the z profile ($R_{\max}$) were also monitored.

Fig. 6 shows the morphology of the surface recorded in both 3D and 2D representations for the films grown by classical PLD (Fig. 6(a)) and UV-assisted PLD (Fig. 6(b)). It is visible that the films grown by UV-assisted PLD are smoother. The roughness parameters determined by WLCM are summarized in Table I.

The films deposited by classical PLD are rougher. We found for this films an average roughness of ~ 250 nm. A decreasing in roughness of more that one order of magnitude is observed for the films deposited under UV illumination.

3.3. Mechanical characterization

Hardness (H) and Young elastic modulus (E) were determined by using a commercially available ultra-low load indentation system, the Nano Indenter® XP (MTS, Corp.), equipped with a Berkovich indenter tip. This highly sensitive mechanical properties microprobe has the capability of sensing both load (P) and displacement (d) continuously as indents are being made in a sample, with resolutions of up to 75 nN and 0.04 nm, respectively. Multiple indentations were made at different loads in the range of 0.5–15 mN. The effective modulus and the hardness have been calculated from using the Oliver–Pharr model [15].

Fig. 7 presents the load–displacement curves obtained at a maximum load of 2.5 mN for the PLD and UV-assisted PLD films. The diagram shows that the films deposited by UV-assisted PLD are more resistant. Thus, the penetration depth of the indentor tip is ~ 180 nm for the PLD film, while for that grown by UV-assisted PLD the depth decrease at ~ 125 mN.

Fig. 8 illustrates the evolution of nano-hardness (a) and Young modulus (b) in the depth of the PLD and UV-assisted PLD film structure.

The PLD films have good mechanical properties. However, the UV-assisted PLD films are harder. Values of hardness and Young modulus of 6–7 and 150–170 GPa, respectively, unusually high for the calcium phosphates, were measured.

The values of hardness (H) and Young modulus (E) measured for the films were presented in Table II. Here, H_a and E_a are the average hardness and Young modulus, respectively.

Fig. 9 illustrates the curve of resistance at the tip penetration traced for the both type of films. The diagram represents the maximum penetration depth in function of the applied load. It confirms that the film grown by classical PLD is less resistant. Thus, for this film the tip penetration depth is ~ 500 nm at 10 mN load, while for

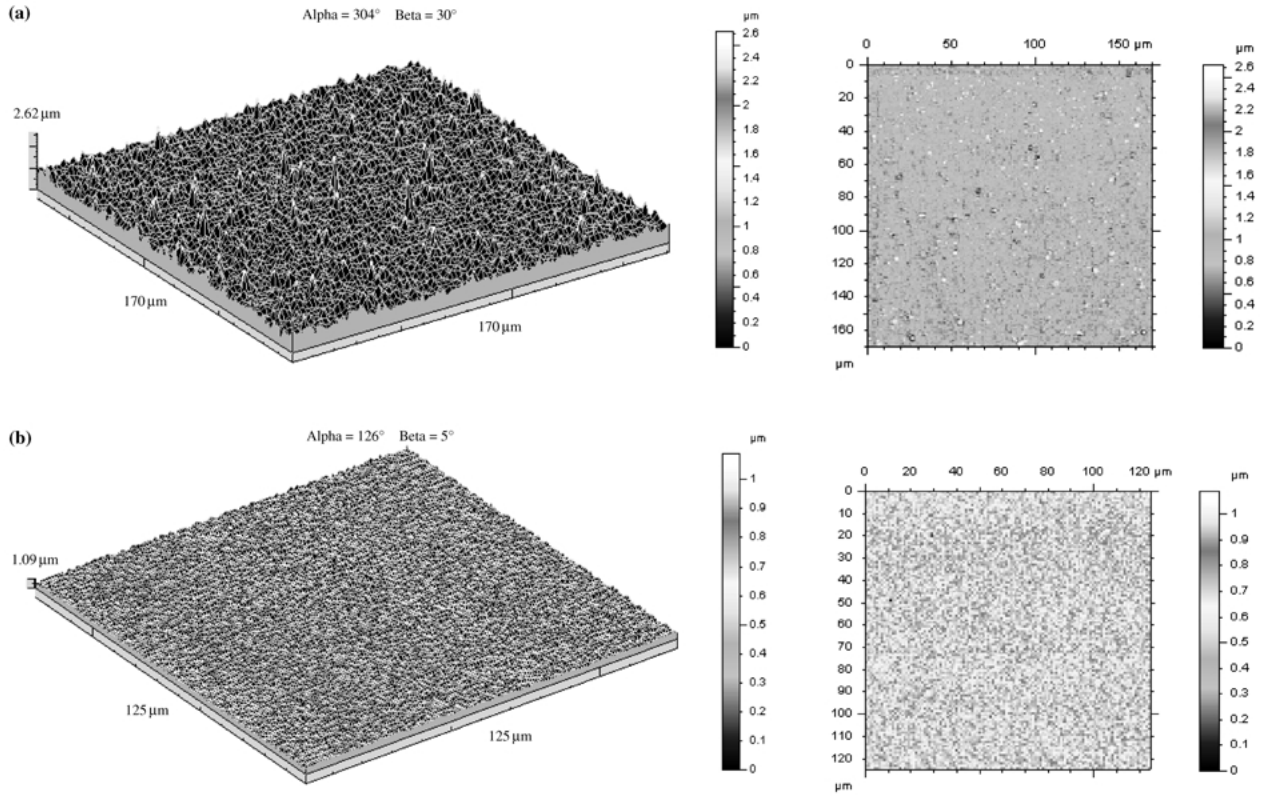

Figure 6 Imaging of the surface topography determined by white light confocal microscopy for the films grown by PLD (a) and UV-assisted PLD (b).

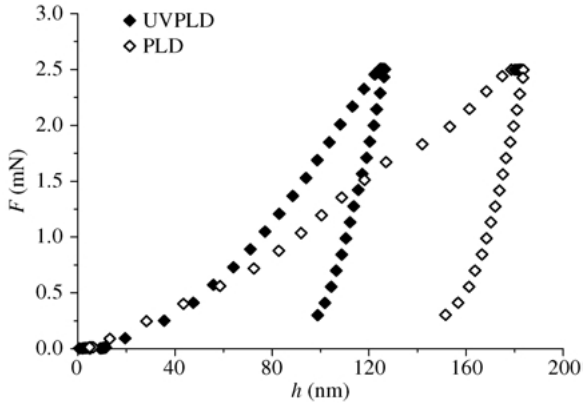

Figure 7 Load–displacement curves obtained at a maximum load of 2.5 mN for the PLD and UV-assisted PLD films.

films grown by UV-assisted PLD, that is reduced at ~ 300 nm.

These results show that the films grown under UV irradiation seem to be more compact. The remarkable mechanical characteristics measured by nano-indentation are assimilated to a denser film microstructure formed during UV illumination.

4. Discussion

The structural analyses show that during the UV-assisted PLD film processing the hydroxyapatite structure of the target is decomposed. This could be explained by the photodissociation of HA molecule simultaneously with the molecular oxygen in laser plasma under UV irradiation by the lamp. In fact, due to the small chemical bonding of –OH hydroxyl group in the HA molecule, the UV radiation could easily produce anhydrous CaP phases. In addition, the H atoms are very light and they can be easily expulsed from the material target and plasma.

A very probable chemical route of HA decomposition could be:

$$Ca_{10}(PO_4)_6(OH)_2 - H_2O \rightarrow Ca_4O(PO_4)_2 + Ca_2P_2O_7 + 4CaO + P_2O_5\uparrow$$

This route is in agreement with the depletion in phosphorous observed from structural analyses. The depletion is made most probably by the volatilization of the phosphorous pentaoxide during film processing.

Conversely, the PLD films contain uniquely HA. The presence at the interface of a TiN buffer layer prevents the eventual contamination of the film by atoms or ions released from the metallic substrate. Moreover, the results of the UV-assisted PLD films confirm that the inserting of buffer layers at the ceramic–metallic interface represents really a challenge for best HA films deposition.

However, despite this undesired HA decomposition, the using of UV irradiation which increase the gas reactivity and atoms mobility, allows to work at very low pressure of gases in the deposition chamber. This enhances the bombardment of the film by the energetic

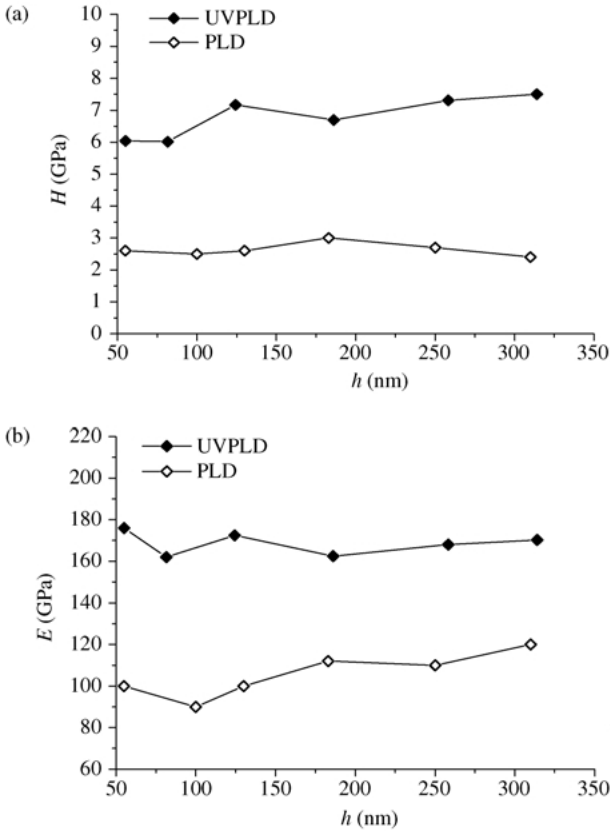

Figure 8 Evolution of the nano-hardness (a) and Young elastic modulus (b) into the depth of the films grown by PLD and UV-assisted PLD techniques.

species of plasma, beneficial upon the general film properties.

As a sign of the improvement of atoms mobility, the atoms and ions arrived at the substrate were found sites with minimal surface energy. Thus, almost all sites in the crystalline network were occupied and the films are dense. Moreover, the UV lamp irradiation can induce defaults destroying and/or recrystallization. Thus, the films are very compact and have excellent mechanical properties. The tensile strength between the film's grains and the bonding strength at the CaP film–substrate interface were increased.

However, the use of the UV irradiation, which allows obtaining these remarkable properties of resistance and solidity of films, is in the detrimental preservation of HA.

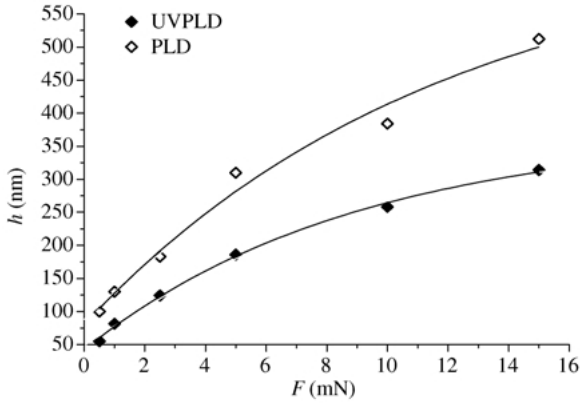

Figure 9 Curve of resistance at the tip penetration of PLD and UV-assisted PLD films.

5. Conclusions

We have investigated the ability of two methods, pulsed laser deposition and *in situ* assisted ultraviolet-pulsed laser deposition to produce crystalline and mechanical resistant calcium phosphate, including hydroxyapatite films. PLD allows creating highly crystalline, stoichiometric and mechanically resistant HA films on Ti-based alloy substrates. The best PLD results were obtained when a TiN buffer layer was inserted at the film–substrate interface. We have demonstrated that the UV-assisted PLD is a technique capable to synthesize CaP films with uncommonly high mechanical resistance, hardness and Young modulus. The UV *in situ* irradiation enhances the gas reactivity and increases the bombardment of surface film with excited species from the laser plasma. These effects proved beneficial for the film densification and tensile bond increasing with the substrate. However, the use of the UV irradiation, which allows obtaining these remarkable properties of resistance and solidity of films, is detrimental in preservation of HA stoichiometry.

Acknowledgments

V.N., M.I., I.N.M., C.R. and J.W. acknowledge with many thanks the financial support to this work by the European Commission through the SIMI project ''Surface Improvement of Metal Implants: new preparation methods and new materials'' (G5RD-CT-2000-00423).

References

1. J. F. OSBORN, in ''Bioceramics'', edited by H. Oenishi, H. Aoki, K. Sawai, (Ishiyaku EuroAmerica Inc., 1989) 388.
2. H. ZENG, W. R. LACEFIELD, S. MIROV, *J. Biomed. Mater. Res.*, **50** (2000) 248.
3. Y. C. TSUI, C. DOYLE, T. W. CLYNE, *Biomater.* **19** (1998) 2015.
4. Y. C. TSUI, C. DOYLE, T. W. CLYNE, *ibid.* **19** (1998) 2031.
5. Pulsed Laser Deposition of Thin Films, edited by D. B. Chrisey and G. K. Hubler, (Wiley, New York, 1994).
6. C. M. COTELL, in Pulsed Laser Deposition of Thin Films, D. B. Chrisey and G. K. Hubler, (Wiley, New York, 1994) 549.
7. M. JELINEK, V. OLSAN, L. JASTRABIK, V. STUDNICKA, V. HNATOWICZ, J. KVITEK, V. HAVRANEK, T. DOSTALOVA, I. ZERGIOTI, A. PETRAKIS, E. HONTZOPOULOS, C. FOTAKIS, *Thin Solid Films* **257** (1995) 125.
8. J. M. FERNANDEZ-PRADAS, M. V. GARCIA-CUENCA, L. CLERIES, A. G. SARDIN, J. L. MORENZA, *Appl. Surf. Sci.* **186** (2002) 1.
9. V. NELEA, C. RISTOSCU, C. CHIRITESCU, C. GHICA, I. N. MIHAILESCU, H. PELLETIER, P. MILLE, A. CORNET, *ibid.* **168** (2000) 127.
10. V. NELEA, H. PELLETIER, D. MULLER, N. BROLL, P. MILLE, C. RISTOSCU, I. N. MIHAILESCU, *ibid.* **186** (2002) 483.
11. D. L. BAULCH, R. A. COX, R. F. OHAMPSON JR., J. A. KERR, J. TROE, R. T. WATSON, *J. Phys. Chem. Ref. Data* **9** (1980) 295
12. I. W. BOYD, J. Y. ZHANG, *Nucl. Instrum. Meth. Phys. Res. B* **121** (1997) 349
13. V. CRACIUN, R. K. SINGH, *Appl. Surf. Sci.* **168** (2000) 239
14. J. COHEN-SABBAN, *Mesures* **179** (1999) 85
15. W. C. OLIVER, G. M. PHARR, *J. Mat. Res* **7**(6) (1992) 1564

Received 24 May
and accepted 29 May 2002